CHAOS
Theory and Applications
in Applied Sciences and Engineering

e-ISSN: 2687-4539
RESEARCH ARTICLE
Vol.6 / No.2 / 2024 / pp.73-82
Special Issue (EDIESCA 2023)
https://doi.org/10.51537/chaos.1376123

Predicting Tipping Points in a Family of PWL Systems: Detecting Multistability via Linear Operators Properties

J.L. Echenausía-Monroy [§,1], **J.R. Cuesta-García** [§,2], **H.E. Gilardi-Velázquez** [α,3], **Sishu Shankar Muni** [β,γ,4] **and J. Álvarez** [§,5]

[§]Applied Physics Division, Center for Scientific Research and Higher Education at Ensenada, CICESE. Carr. Ensenada-Tijuana 3918, Zona Playitas, Ensenada, 22860, B. C., Mexico, [α]Facultad de Ingeniería, Universidad Panamericana. Josemaría Escrivá de Balaguer 101, Aguascalientes, Aguascalientes, 20296, Mexico, [β]School of Digital Sciences, Digital University Kerala, Technocity campus, Mangalapuram, Kerala, India, [γ]Indian Institute of Information Technology and Management Kerala, Technopark road, Kerala, India.

ABSTRACT The study of dynamical systems is based on the solution of differential equations that may exhibit various behaviors, such as fixed points, limit cycles, periodic, quasi-periodic attractors, chaotic behavior, and coexistence of attractors, to name a few. In this paper, we present a simple and novel method for predicting the occurrence of tipping points in a family of Piece-Wise Linear systems (PWL) that exhibit a transition from monostability to multistability with the variation of a single parameter, without the need to compute time series, i.e., without solving the differential equations of the system. The linearized system of the model is analyzed, the stable and unstable manifolds are taken to be real vectors in space, and the changes suffered by these vectors as a result of the modification of the parameter are examined using such simple metrics as the magnitude of a vector or the angle between two vectors in space. The results obtained with the linear analysis of the system agree well with those obtained with the numerical resolution of the dynamical system itself. The work presented here is an extension of previous results on this topic and contributes to the understanding of the mechanisms by which a system changes its stability by fragmenting its basin of attraction. This, in turn, enriches the field by providing an alternative to numerical resolution to identify quantitative changes in the dynamics of complex systems without having to solve the differential equation system.

KEYWORDS
Nonlinear dynamics
Chaotic system
Multistability
PWL system
Bifurcation
Tipping point

INTRODUCTION

In a world governed by complex systems that describe behaviors as mundane as our social interactions to the interconnected workings of our brains as the control center of the human body, the ability to anticipate the moment when a system reaches a point of no return is critical (Scheffer *et al.* 2001; Lenton *et al.* 2008; Jung and Ager 2023). This is a strategic advantage that can be applied to a wide range of disciplines. In this context, we should think of a complex system as an entity consisting of multiple parts whose individual behavior is known and which interact with each other. The behavior of the complex system, in turn, is not equal to the sum of the behaviors of the individual parts, resulting in structures that are generally characterized by nonlinearities (Ott 2002; Echenausía-Monroy *et al.* 2022; Keleş *et al.* 2023).

In the study and characterization of dynamical systems lies one of the central problems: exploring the asymptotic properties of the model when the parameter is continuously changed (Guan *et al.* 2005). A variety of behaviors that a dynamical system can exhibit include equilibrium points, limit cycles, periodic oscillations, chaotic behavior, quasi-periodic behavior, and even the coexistence of attractors can occur, to name a few examples (Ott 2002; Awal and Epstein 2021).

Even if a system exhibits only one type of behavior, the continuous change of system parameters or the influence of external disturbances can lead the system to the point of no return mentioned above. This point is called *tipping point*, where the dynamic behavior of the system changes abruptly and sometimes irreversibly (Biggs *et al.* 2009; Lane 2011). These two types of bifurcations can

Manuscript received: 15 October 2023,
Revised: 18 November 2023,
Accepted: 22 November 2023.

[1]echenausia@cicese.mx (**Corresponding author**)
[2]jcuesta@cicese.mx
[3]hgilardi@up.edu.mx
[4]sishushankarmuni@gmail.com
[5]jqalvar@cicese.mx

be distinguished from a bifurcation point because the tipping point refers to an abrupt and irreversible change in dynamic behavior. In contrast, the bifurcation point can describe changes in equilibrium points, for example, but does not necessarily imply a dynamic change. Examples of this type of abrupt modification in behavior include power outages in electricity grids or the occurrence of massive congestion in urban transportation systems. It is therefore crucial to have tools that allow us to predict the occurrence of these bifurcation points, for example, to make public health decisions regarding the spread of a disease that could lead to a pandemic, to predict a financial crisis, or to measure the tolerance of an ecosystem on the verge of collapse (Rial *et al.* 2004; Jiang *et al.* 2019; O'Regan *et al.* 2020; Lohmann *et al.* 2021; Wunderling *et al.* 2023).

Such a change in parameters in a complex system can lead to transitions between different behaviors, for example, a double limit cycle can bifurcate into the occurrence of chaotic states. These transitions may also involve the occurrence of coexisting states, which is referred to as multistability (Gilardi-Velázquez *et al.* 2018; Echenausía-Monroy *et al.* 2020; Fang *et al.* 2022; Safavi and Dayan 2022). This nearly universal phenomenon describes a range of behaviors from optical illusions to chemical reactions, the use of words, and even emotions. The coexistence of states in complex systems entails the existence of more than one basin of attraction. For a given parameter of the system, the dynamics may oscillate at near of a stable attractor (equilibrium points, periodic orbit, chaotic attractor) for certain initial conditions, but converge to another for a different set of, albeit very similar, initial conditions.

Since Lorenz's work (Lorenz 1963), many research has been done on how to characterize and find the existing behaviors in a dynamic system with complex behavior. One of the most commonly used forms for this is bifurcation diagrams, both for the existence of fixed points and for changes in their stability, but describing only local behaviors. In the case of systems with complex behavior, there are no tools that allow to describe the types of behavior through the analysis of vector fields, but only through the analysis of time series (Nazarimehr *et al.* 2018).

Currently, the search for new ways to predict tipping points in dynamical systems has attracted the attention of the scientific community, as it is seen as an advantage for decision making in critical situations (Moore 2018; Peng *et al.* 2019). In this search and the development of techniques capable of anticipating the occurrence of abrupt dynamic changes, tools based on the analysis of time series are used. This technique is based either on the storage of time series of the phenomenon under study or on the system of equations that describes it. Various statistical and mathematical techniques are used to detect patterns, trends, or changes in the behavior of the system that may indicate that the dynamic behavior is approaching a tipping point. In these cases, early warning signals may be observed, such as increased variance, autocorrelation, or a slowing of recovery rates in response to system perturbations, also known as resilience (Nazarimehr *et al.* 2018; Chen *et al.* 2020; Moghadam *et al.* 2022). Bifurcation theory has also been used to study how the qualitative behavior of a system changes as its parameters vary. By analyzing bifurcation points, it is possible to identify critical thresholds at which inflection points are likely to occur. Similarly, the use of Lyapunov exponents is a popular tool for identifying when a dynamical system is about to change its behavior (Tsakonas *et al.* 2022).

In some cases where the descriptor model leads to a numerical simulation with high computational costs, surrogate or reduced-order models can be used to approximate the behavior of the system and predict inflection points, just as network-based approaches have been used to detect changes in the network structure that might indicate an impending tipping point (Jiang *et al.* 2018).

Although there is a wealth of literature with different approaches to identifying and predicting tipping points in dynamical systems, in most cases there is one constant: time series analysis, which is effective but involves a high computational cost. We have recently published a paper that addresses the prediction of inflection points in a single-parameter Piece Wise Linear (PWL) system that generates multiple scrolls based on the study of the linear operator of the system. This approach shows a relation between vector field properties and the occurrence of coexisting states, with which is possible to predict the tipping points when the system undergoes a change in its global stability due to the variation of one parameter, which causes the system to go from monostability to multistability. The method described in (Echenausía-Monroy *et al.* 2022b) is based on the study of the stable and unstable manifolds of the system as real vectors in three-dimensional space which characterizes the changes in their magnitudes so that the points at which an abrupt change in the dynamics of the system can be identified. While the results are interesting, they are limited to a monoparametric family of attractors that are not able to predict the emergence of multistable dynamics in a system like the one published in (Gilardi-Velázquez *et al.* 2017), where the multi-scroll system has three distinct parameters.

In the present work, the results shown in (Echenausía-Monroy *et al.* 2022b) are generalized to a multiparametric family of oscillators, which are described by three dynamical parameters that change the size, order, and the Lyapunov exponent of the dynamics. In this paper, metrics of vector fields such as the magnitude of a vector and the angle between two vectors in space are used to characterize the variations of real vectors associated with the varieties of the multiple scroll system. The proposed method allows the prediction of tipping points through the eigenspace associated to the vector field, *i.e.*, without the need to solve the system of differential equations, which brings a significant reduction in computational costs. Since the numerical resolution of the system is eliminated, these results can be extended to systems with a larger number of variables without increasing the computational cost.

The remainder of the work consists of the following sections: Section 2 presents the necessary groundwork used in this paper and delineates the problem to be solved. Section 3 describes the methodology used, while the results are discussed in Section 4. The conclusions are explained at the end of the work.

PRELIMINARIES

Consider a third-order Piece-Wise Linear system defined as follows:

$$\dot{\boldsymbol{X}} = \boldsymbol{M}\boldsymbol{X} + g(\boldsymbol{X}), \tag{1}$$

where $\boldsymbol{M}$ is a non-singular linear operator, $\boldsymbol{X}$ is the state vector, $g : \mathbb{R}^n \to \mathbb{R}^n$ is a real commutation function based on a state variable and defined for a set of constant vectors as shown in Eq. (2), where $B_i = [b_1, \ldots, b_l] \in \mathbb{R}^n$ for $h = 1, 2, \ldots, l$ is a set of vectors with real entries. On the other hand, $\Omega_1, \ldots, \Omega_l$ denote a polytopic partition of the state space, also called switching domains, such that $\bigcup_{h=1}^{l} \Omega_h = \mathbb{R}^n$ and $\Omega_h \bigcap (\Omega_m)^0 = \emptyset$, where the notation $(\Omega_m)^0$ denotes the interior of Ω_m. Moreover, in each domain $\Omega_h \subset \mathbb{R}^n$, the system has equilibrium points located at $\boldsymbol{\chi}_h^* = -\boldsymbol{M}^{-1} g(\boldsymbol{X})$,

where $\boldsymbol{M}$ is the linear operator of the system, and it is easy to see that there are as many equilibria as domains Ω_h.

$$g(\boldsymbol{X}) = \begin{cases} B_1 & \text{if} \quad \boldsymbol{X} \in \Omega_1, \\ B_2 & \text{if} \quad \boldsymbol{X} \in \Omega_2, \\ \vdots & \vdots \\ B_l & \text{if} \quad \boldsymbol{X} \in \Omega_l. \end{cases} \tag{2}$$

The interest of this work is to characterize the behavior of PWL systems with the same number of scrolls as equilibrium points. To this end, the eigenvalues of *Eq. (1)* must be described by an Unstable Dissipative System type 1 (UDS I) (Campos-Cantón *et al.* 2010; Campos-Cantón 2015), characterized by having unstable saddle points for the following conditions:

- The linear operator $\boldsymbol{M}$ must have a negative real eigenvalue and a pair of complex conjugates with a real positive component.
- The eigenvalues $\boldsymbol{\lambda} \in \mathbb{C}^{1\times 3}$ of $\boldsymbol{M}$ must satisfy: $\sum_{i=1}^{3} \lambda_i < 0$.

Under these conditions, this article examines a jerk-inspired oscillator generated by:

$$\boldsymbol{M} = \begin{bmatrix} 0 & 1 & 0 \\ 0 & 0 & 1 \\ -\alpha_1 & -\alpha_2 & -\alpha_3 \end{bmatrix}, \ \boldsymbol{X} = \begin{bmatrix} x_1 \\ x_2 \\ x_3 \end{bmatrix}, \ g(\boldsymbol{X}) = \begin{bmatrix} 0 \\ 0 \\ \alpha_1 b(x_1) \end{bmatrix}, \tag{3}$$

$$b(x_1) = \begin{cases} -2 & \text{if} \quad \boldsymbol{X} \in \Omega_1 = \{\boldsymbol{X} \in \mathbb{R}^n : x_1 < -1\}, \\ 0 & \text{if} \quad \boldsymbol{X} \in \Omega_2 = \{\boldsymbol{X} \in \mathbb{R}^n : -1 \leq x_1 < 1\}, \\ 2 & \text{if} \quad \boldsymbol{X} \in \Omega_3 = \{\boldsymbol{X} \in \mathbb{R}^n : x_1 \geq 1\}, \end{cases} \tag{4}$$

where x_i are the state variables, α_i, $i = 1, 2, 3$ are the dynamical parameters corresponding to the family of oscillators that also modify the Lyapunov exponent, the order and the size of the attractor (Echenausía-Monroy *et al.* 2018), where $b(x_1)$ is a function that generates a commutation based on a state variable that induces multiple scrolls in the x_1-dimension.

Since this work focuses on the system responding to the configuration of eigenvalues defined as UDS I, which in turn are defined by the combination of the system parameters, mathematical analysis as described in (Anzo-Hernández *et al.* 2018) is used to determine the proper values:

Proposition 1 *(Anzo-Hernández* et al. *2018) Consider the family of affine linear systems given by Eq. (1,3), and the linear operator $\boldsymbol{M}$ with parameters $\alpha_1, \alpha_2, \alpha_3 \in \mathbb{R}^+$. If $\alpha_1 > 0, 0 < \alpha_2 < \frac{\alpha_1}{\alpha_3}$, and $\alpha_3 > 0$, then the system described by Eqs. (1,3) is based on an Unstable Dissipative System type 1 (UDS-I).*

Proof 1 *(Anzo-Hernández* et al. *2018) Suppose that $\alpha_1, \alpha_2 > 0$. Since $\alpha_3 = Trace(\boldsymbol{M}) = \sum_{i=1}^{3} \lambda_i < 0$, where λ_i, $i = 1, 2, 3$, is each of the eigenvalues of $\boldsymbol{M}$, the system Eq. (1,3) is dissipative. Moreover, with $\alpha_1 = det(\boldsymbol{M})$, the system Eq. (3) has saddle equilibrium points determined by the characteristic polynomial of the linear operator $\boldsymbol{M}$, $\lambda^3 + \alpha_3\lambda^2 + \alpha_2\lambda + \alpha_1 = 0$, which for $\alpha_2 < \frac{\alpha_1}{\alpha_3}$ by the Hurwitz polynomial criterion implies instability. Since α_1, α_2 and α_3 are positive real constants and the characteristic polynomial has no positive characteristic values by Descartes' sign rule, it has only one negative eigenvalue by which the equilibrium point is saddle fixed. Then the eigen spectrum is given by a negative real eigenvalue and a pair of complex conjugate eigenvalues with a positive real part.*

Considering Proposition 1, a multi-scroll jerk inspired system with parameters $\alpha_1 = 10.5$, $\alpha_2 = 7$; $\alpha_3 = 0.7$ for Eq. (3) and the commutation function described by Eq. (4) satisfies the UDS I conditions, generating the attractor shown in Figure 1. The red dots indicate the location of the equilibrium point, and the vertical lines indicate the location of the commutations delimiting each of the system domains, or polytopic partitions.

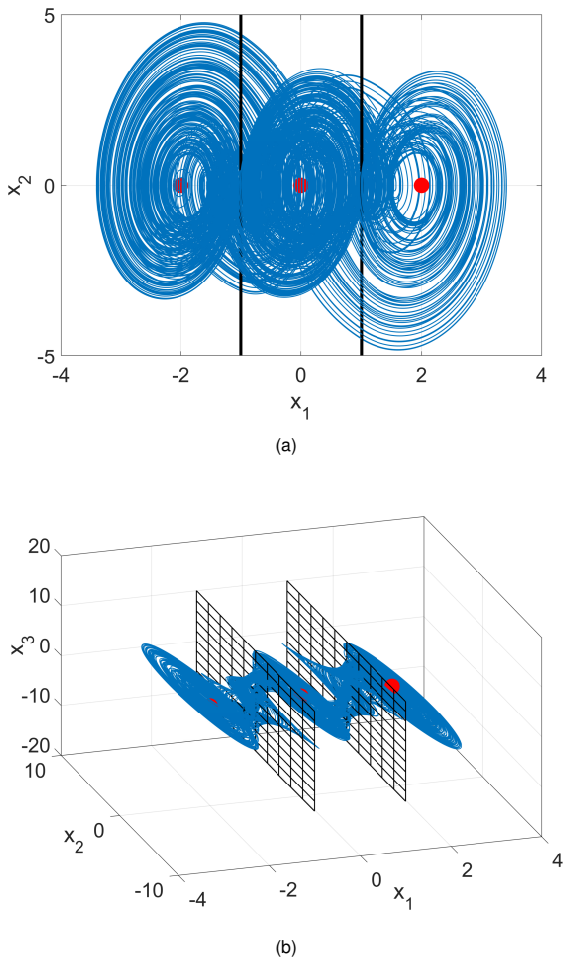

Figure 1 Attractor generated by Eq. (3) and Eq. (4) for $\alpha_1 = 10.5$, $\alpha_2 = 7$; $\alpha_3 = 0.7$ seen in the projection (a) $x_1 - x_2$ and (b) in phase space. The red dots denote the equilibrium points, while the black vertical lines (plane) represent the commutation surfaces.

Remark 1 *Note that the α_i values used in Figure 1 are the same as described in (Gilardi-Velázquez* et al. *2017), but with a restricted commutation function, since the authors use the "round to the nearest integer" function as commutation law in the work described, generating an infinite number of equilibrium points.*

In (Gilardi-Velázquez *et al.* 2017), the authors show that a multi-scroll system like the one described in Eq. (3) (for $\alpha_1 = 10.5$, $\alpha_2 = 7$, $\alpha_3 = 0.7$) is able to go from monostability to multistability by changing a bifurcation parameter that affects the third equation of the descriptor system. The resulting system of equations is shown in Eq. (5), where the parameter μ is a positive constant that scales with the dynamical parameters of the system, changing its stability and allowing the transition between monostability and the coexistence of stable single-wing attractors.

$$\begin{aligned} \dot{x_1} &= x_2, \\ \dot{x_2} &= x_3, \\ \dot{x_2} &= \mu[-\alpha_1 x_1 - \alpha_2 x_2 y - \alpha_3 x_3 + \alpha_1 b(x_1)]. \end{aligned} \tag{5}$$

Through numerical simulations, it is possible to identify the points at which the system changes its global stability by fragmenting its basin of attraction, from the generation of a 3-scroll attractor (as in Figure 1) to the generation of a single-wing attractor capable of living stably at each of the equilibrium points of the system. If we use a bifurcation diagram, by μ variation (see Figure 2(a)), and count the number of scrolls that the dynamics generates by changing the parameter μ, we obtain the graph shown in Figure 2(b), where the starting point of the multistable dynamics is $1.03 \leq \mu \leq 2.14$. For $\mu \geq 2.14$, all dynamics are eliminated from the system and converge to the equilibrium point.

Remark 2 *Although the results shown in Figure 2 are not identical to those previously published in (Gilardi-Velázquez* et al. *2017), they are not the main result of this work, but they are necessary to understand the contribution of the paper, which is why they are kept in the Preliminary remarks section.*

Problem Statement

In our previous study (Echenausía-Monroy *et al.* 2022b), we presented an innovative approach to predict tipping points in Piece Wise-Linear (PWL) systems by using linear algebra techniques to analyze the magnitude of manifolds within a monoparametric family of oscillators ($\alpha_1 = \alpha_2 = \alpha_3$). The focus of that research was primarily on identifying these tipping points for a particular class of oscillators. In this current work, we have extended, refined our methodology and generalized its applicability to multiparametric families of multi-scroll PWL oscillators. Our main goal remains the same: to predict the occurrence of tipping points in PWL systems transitioning from monostability to the occurrence of multistable behavior without the need to compute time series, i.e., without solving the differential equations of the system. To achieve this, we have developed an innovative approach that analyzes the angular relationships between real vectors associated with stable and unstable manifolds.

This study builds on our previous research, but it is important to emphasize that the problem, while conceptually related, applies to a broader range of dynamical systems. We improve and generalize the methodology so that it is applicable to different families of multiparametric oscillators. This advance is crucial to gain deeper insights into the transition from monostability to multistability in complex systems without relying on numerical resolution or bifurcation parameter change detection.

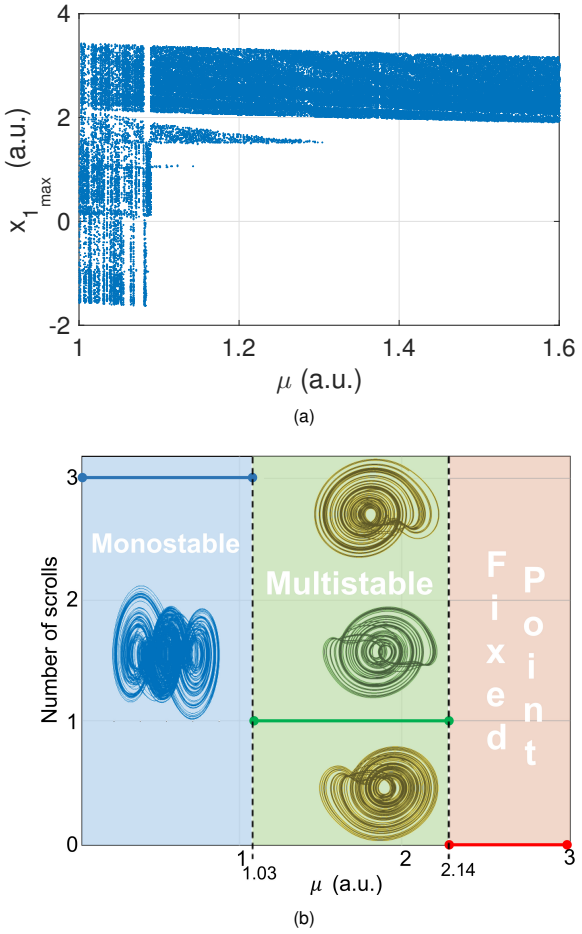

Figure 2 Numerical simulation of the system described by Eqs. (4,5) for $\alpha_1 = 10.5$, $\alpha_2 = 7$; $\alpha_3 = 0.7$ by μ variation. (a) Bifurcation diagram of the local maxima in x_1 by tracking the attractor (using the final state as the initial condition for parameter variation for the initial conditions $x_i = [-0.1\ 0.1\ 0.1]'$). (b) Summary of the behavior shown in the bifurcation diagram.

METHODOLOGY

Matrix algebra, or linear algebra as it is treated in college textbooks, focuses on the study and manipulation of algebraic structures called *vectors* and *matrices*. At its core, it deals with the properties and operations associated with these objects and is used to solve a variety of problems in fields ranging from physics and engineering to computer science and statistics. It has its origins in civilizations such as the Babylonians and Greeks, who were concerned with problems of systems of linear equations by matrix representation, and developed into a mathematical discipline with the contributions of notable mathematicians such as Leonhard Euler and Joseph-Louis Lagrange (Kleiner 2007).

As mentioned in the previous sections, the methodology used in this paper is based on the notion of the changes suffered by the stable and unstable manifolds of the multi-scroll system, which are conceived as real vectors in space. By conceptualizing them as vectors in space, we can quantify their changes by examining their magnitude and the angle that exists between these in the plane or in space.

The determination of the manifolds and their subsequent con-

struction as vectors is done using the linear operator of the descriptor system by computing the eigenvalues and eigenvectors of the model, graphing them in space, and determining their three-dimensional coordinates. As example, and considering Proposition 1, a multi-scroll jerk inspired system with parameters $\alpha_1 = 10.5$, $\alpha_2 = 7$, $\alpha_3 = 0.7$, $\mu = 1$ for Eq. (5) and the commutation function described by Eq. (4) satisfies the UDS I conditions, generating the attractor shown in Figure 1. For this combination of α_i values, the linear system to study is described by Eq. (6), being its eigenvalues described in (7):

$$\boldsymbol{M} = \begin{bmatrix} 0 & 1 & 0 \\ 0 & 0 & 1 \\ -\mu\alpha_1 & -\mu\alpha_2 & -\mu\alpha_3 \end{bmatrix}, \tag{6}$$

$$\begin{aligned} \Lambda &= \{\lambda_{1,2,3}\}, \\ &= \{-1.3372, 0.3186 \pm 2.784\,\mathrm{i}\}, \end{aligned} \tag{7}$$

and their corresponding eigenvectors are equal to:

$$\begin{aligned} \vartheta &= \{\vartheta_{1,2,3}\}, \\ &= \left\{ \begin{pmatrix} 0.4087 \\ -0.5466 \\ 0.7309 \end{pmatrix} \begin{pmatrix} -0.1160 \pm 0.0269\,\mathrm{i} \\ 0.0379 \pm 0.3316\,\mathrm{i} \\ 0.9351 \end{pmatrix} \right\}. \end{aligned} \tag{8}$$

The stable and unstable manifolds of the multiscroll system are defined such that $\vartheta = [\vartheta_i]$, for $i = 1, 2, 3$ is a set of column eigenvectors, where $\boldsymbol{M}\vartheta_i = \lambda_i\vartheta_i$, where λ_i are the system eigenvalues. Under this assumption, the stable manifold is defined by E_s^* =Span$\{\vartheta_1\}$ and the unstable manifold by E_u^* =Span$\{\vartheta_{2,3}\}$, and to represent these manifolds, we consider the real part of both as $E_s = \mathrm{Re}\{E_s^*\}$ and $E_u = \mathrm{Re}\{E_u^*\}$. With this in mind, it is possible to plot the attractor shown in Figure 1 along with the real vectors associated with the stable and unstable manifolds as shown in Figure 3.

Note that Figure 3 shows both manifolds (E_u, E_s) as real vectors in space that always intersect the equilibrium point and are bounded by the commutations induced by the nonlinear function. Under this premise, it is possible to analyze the behavior of these vectors by characterizing their variation and calculating their magnitude change induced by the parameter μ in the system. For this purpose, consider the points A, B, C, and D (see Fig. 3(b)), which have three-dimensional coordinates, intersections with the commutation surfaces, and intersections with the equilibrium point; the associated real vectors can be constructed as follows:

$$\begin{aligned} \vec{M}_s &= \vec{DB} = D - B, \\ \vec{M}_u &= \vec{AC} = A - C, \end{aligned} \tag{9}$$

where the vectors associated with both manifolds have coordinates in space and their magnitude is then defined as:

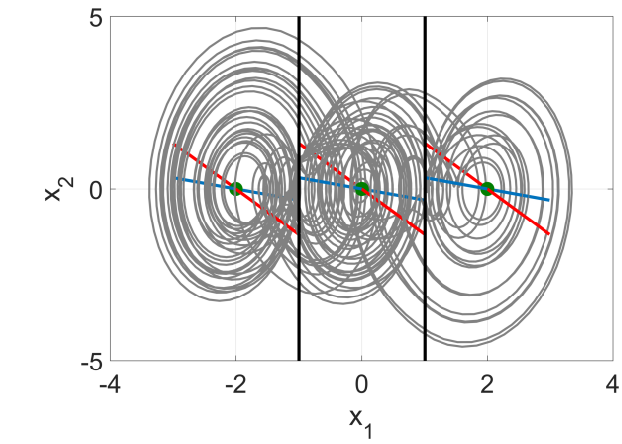

(a)

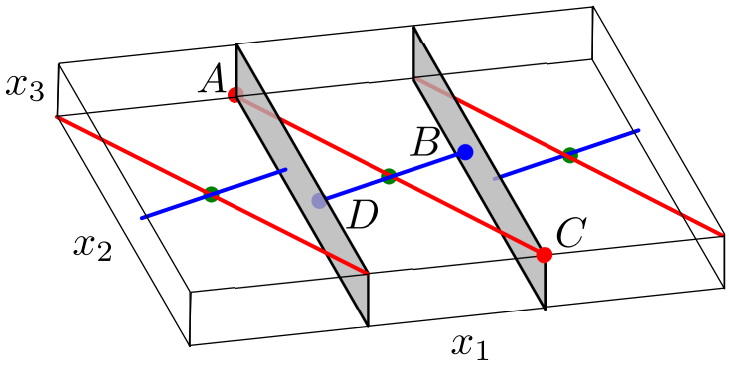

(b)

Figure 3 (a) Attractor generated by Eq. (3,5) for $\mu = 1$, $\alpha_1 = 10.5$, $\alpha_2 = 7$, $\alpha_3 = 0.7$, where the real vector associated with the stable manifold is shown in blue and the one associated with the unstable manifold is shown in red. (b) Real vectors associated with the system manifolds in phase space, omitting the trajectory shown in (a).

$$\begin{aligned} ||\vec{M}_s|| &= \sqrt{(x_{1s_1} - x_{1s_2})^2 + (x_{2s_1} - x_{2s_2})^2 + (x_{3s_1} - x_{3s_2})^2}\,, \\ ||\vec{M}_u|| &= \sqrt{(x_{1u_1} - x_{1u_2})^2 + (x_{2u_1} - x_{2u_2})^2 + (x_{3u_1} - x_{3u_2})^2}\,. \end{aligned} \tag{10}$$

In the same way as for the magnitude of the real vectors associated with the stable and unstable manifolds, it is possible to calculate the cross product between these vectors, defined as shown in Eq. (11), where θ is the angle between the vectors $\vec{M}_s$ and $\vec{M}_u$.

$$||\vec{M}_s \times \vec{M}_u|| = ||\vec{M}_s||\,||\vec{M}_u||\sin(\theta), \tag{11}$$

Remark 3 *Both metrics described previously, the magnitude of the vectors described in Eq. (10) and the cross product between the vectors shown in Eq. (11), are defined for a set of parameters α_i and μ. In this work, the variations of the two metrics are analyzed based on the effect induced by the bifurcation parameter μ, and these variations are illustrated in Figure 4.*

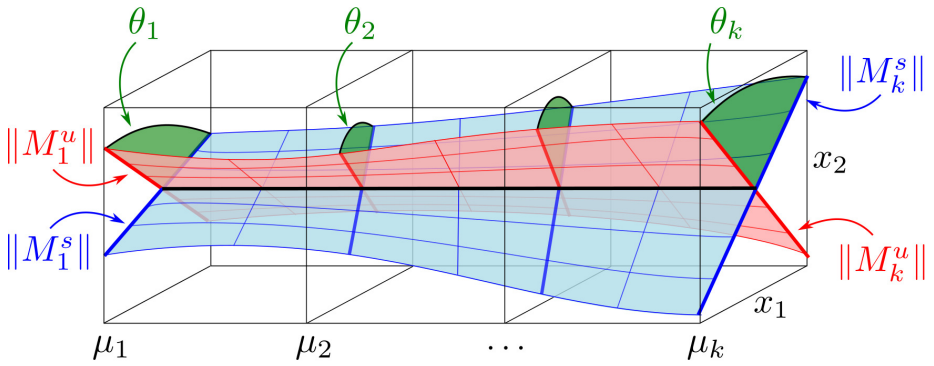

Figure 4 Illustration of the variations of the real vectors associated with the stable and unstable manifolds as the parameter μ changes, considering the vector magnitude ($||\vec{M}_{u,s}||$) and the angle between vectors (θ).

In addition, Appendix A presents an analytical method for characterizing the angles between real vectors in the system. This approach uses both the eigenvalues and the eigenvectors of the system under analysis.

RESULTS AND DISCUSSION

In the same spirit that (Echenausía-Monroy *et al.* 2022b), the eigenspace changes are analyzed along the variation of the parameter μ in the linear operator of the system described by Eq. (5). For each value of μ, the real vectors associated with the stable and unstable manifolds are computed, and in turn, the magnitude of these vectors is calculated. These changes are plotted (for both the stable and unstable manifolds), and points are searched for where these curves intersect. The intersections describe (from what has been reported) the regions where the system shows qualitative changes in its behavior, indicating the occurrence of multistable states, associated with the tipping points in the system. Figure 5 shows the curves obtained for the parametric variations of the magnitudes of the vectors $\vec{M}_s$ (solid lines) and $\vec{M}_u$ (dashed lines). Each of the magnitudes is calculated for the three-dimensional space and in each of the system projections, resulting in 4 curves for each of the vectors.

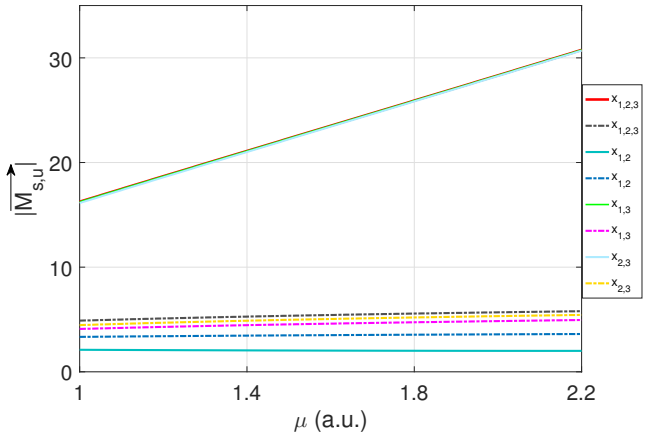

Figure 5 Behavior of the magnitudes of vectors $\vec{M}_s$ and $\vec{M}_u$ throughout the change of parameter μ. The values used are the same as in the attractor in Figure 1 ($\alpha_1 = 10.5$, $\alpha_2 = 7$, $\alpha_3 = 0.7$), and the subindex indicate the projection in which the magnitude is calculated (see Remark 4).

Remark 4 *In the results presented in this section, the notation $x_{\mathbb{I}}$, $\theta_{\mathbb{I}}$ is used, where the subindex $\mathbb{I}$ indicates whether the result was computed in the three-dimensional plane $\mathbb{I} = 1,2,3$ or in one of the state-space projections ($\mathbb{I} = 1,2$, $\mathbb{I} = 1,3$, $\mathbb{I} = 2,3$). Then for each metric used (vector magnitude and angle between vectors) there are 4 values.*

Analyzing the behavior of Figure 5, it becomes clear that there are no intersections in the curves describing the changes in the magnitudes of the real vectors associated with the manifolds of the system under study. The linear operator of the system described by Eq. (5) for the values $\alpha_1 = 10.5$, $\alpha_2 = 7$, $\alpha_3 = 0.7$ serves as a reference point. The absence of the appearance of intersections, as seen in Figure 10 of (Echenausía-Monroy *et al.* 2022b), is due to the fact that in this work we analyze the behavior of the whole family of oscillators described by different parameters α_i. The above mentioned article it was worked with a family of attractors described in the UDS I-value section ($\alpha_1 = \alpha_2 = \alpha_3$), which allows visualization of intersection points between the magnitudes of $\vec{M}_s$ and $\vec{M}_u$ as a function of μ.

In this sense, and maintaining the goal of being able to predict the occurrence of multistable states of the system in the context of a linear analysis without having to analyze the time series, the cross product between vectors is used. This vector operation results in a new vector that is perpendicular to the analyzed vectors. With the vectors $\vec{M}_s$ and $\vec{M}_u$, a perpendicular vector between them is obtained, which in turn gives the angle between the analyzed vectors (θ). This is the value used to characterize the variations of the linear operator, as described in Eq. (11). Figure 6 shows the results obtained by graphing the angle between the vectors of the variations obtained by the cross product. Appendix A presents an analytical method to describe the angles between real vectors within the system. This method relies on both the eigenvalues and eigenvectors of the system under study. It provides an alternative to the visual representation of changes in the system.

Analyzing the behavior of the curves of the angles between the vectors $\vec{M}_s$ and $\vec{M}_u$ in space and in each of the projections, we can identify three intersections. The first one for $\mu = 1.038$; it occurs when the angle between the vectors in both projections $x_{1,2} - x_{1,3}$ reaches the same value, where the plane $x_{1,2}$ is the one where the attractor projection reveals the multistable behavior.

The second intersection point appears for $\mu = 1.158$ when the angle between the vectors reaches the same value for both the projection $x_{1,2}$ and the plane $x_{2,3}$. The last interesting point appears for $\mu = 1.5$ when the angle between the vectors in the three-dimensional space reaches the same value as the angle between the vectors in the plane where the coexistence of the attractors is

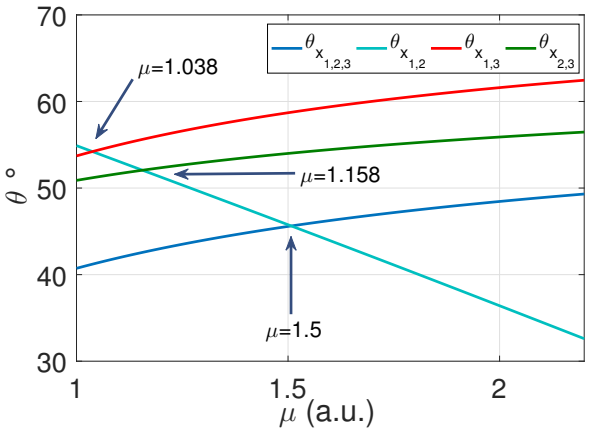

Figure 6 Behavior of the angle between the vectors $\vec{M}_s$ and $\vec{M}_u$ when varying the parameter μ, determined with the cross product. The values used are $\alpha_1 = 10.5,\ \alpha_2 = 7,\ \alpha_3 = 0.7$, which are the same as in the attractor in Figure 1.

appreciated ($x_{1,2}$).

Remark 5 *The first intersection point, where the angles between the varieties converge to the same value, is consistent with what was determined by the analysis of the time series (see Figure 2).*

Comparing the behavior of the angles between the vectors (Figure 6) with the bifurcation diagram shown in Figure 1, we can see that the first intersection between the curves corresponds to the value of μ at which the system breaks its global stability and the coexisting states arise. But it is impossible to ignore the fact that these angular curves have three intersection points. To investigate this behavior, Figure 7 shows the attractors obtained for the values of μ given in the angular curves, where the vectors reach interesting values. The time series used for these figures were calculated for 2^{18} points for an integration step $\tau = 0.01$ with RK4.

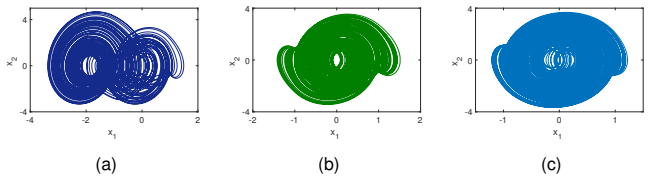

Figure 7 Multistable behavior of the system described by Eqs. (3,5) for the values used corresponds to that of the attractor in Figure 1 $\alpha_1 = 10.5,\ \alpha_2 = 7,\ \alpha_3 = 0.7$ and initial conditions $x_{1i} = -1,\ x_{2i,3i} = 0.1$. (a) $\mu = 1.038$, (b) $\mu = 1.158$, (c) $\mu = 1.5$.

After analyzing the dynamic behavior of the multi-scroll system described by Eqs. (3,5), we can say that the intersection points between the curves of the angles between the vectors correspond to three points where the dynamics of the system undergoes a change, or tipping points:

- $1 < \mu < 1.15$ The system exhibits the coexistence of attractors, but the dynamics is such that there is a basin of attraction with 6 possible attractors, as shown in the (Echenausía-Monroy *et al.* 2022a) obtained by using fractional derivatives. The global monostability has been slightly modified. There is the possibility of i) attractors of a single-wing living in each of the equilibrium points, ii) two symmetric double-scroll attractors, and iii) a small region in the initial conditions for which the system remains monostable.
- $1.15 < \mu < 1.5$ The basins of attraction of the multistable system have become larger, the monostable attractor is almost improbable, and the probability of the occurrence of a double-scroll attractor is small.
- $1.5 < \mu < 2.14$ The system exhibits only the coexistence of attractors of one wing, which live stably in each of the polytopic partitions of the system, which in turn have a single associated equilibrium point.
- $\mu > 2.14$ The system exhibits only the coexistence of stable equilibrium points, in accordance with Proposition 1.

CONCLUSION

The work developed and presented here addresses the problem of predicting the occurrence of inflection points, also called tipping points, in a multi-scroll system moving from monostability to coexistence of attractors. The implemented methodology is based on the study of the linear operator of the descriptor model. Without having to solve the system of equations and/or analyze time series, the points at which the dynamics change such that the coexistence of attractors occurs were predicted.

Using simple techniques of matrix algebra, such as the magnitude of a vector and the cross product between vectors, the linear operator of the system was analyzed. The results obtained are in agreement with those published in other papers on time series analysis. More importantly, considering Proposition 1, the developed method is applicable to the whole family of oscillators described by Eq. (5), and the linear operator depicted in (9). At the same time, it is worth noting that the result can be extrapolated to any number of scrolls in phase space as long as a nonlinear function with equidistant equilibrium points at the center of each of the polytopic partitions is used.

Although the analysis and metrics used are simple and easy to implement, it is worth noting that this allows us to better understand the transition between monostability and coexistence with attractors in dynamical systems. If we develop a tool to relate the angles between the stable and unstable manifolds to the dynamical transitions of the oscillator, then the points where the angles between said manifolds reach the same values in the projection $x_{1,2}$ with the projection $x_{2,3}$ are the points where the system breaks its stability. It is important to emphasize that the projection in which the multistability is estimated is in the plane $x_{1,2}$. It is worth noting that, contrary to what was reported in (Echenausía-Monroy *et al.* 2022b), the methodology proposed in this article is not able to predict the point at which the system changes the stability of its equilibrium points and transforms them into attractive foci points.

In addition, throughout Appendix A, the approach to analytically describe the angle between the real vectors in the system is described by using both the eigenvalues and the eigenvectors of the analyzed system. This is an alternative to the graphical method of visualizing the varieties of the system as real vectors, and enriches the contribution of the paper. It should be emphasized that with the results shown in this paper it is possible to predict the occurrence of multistable states in jerky systems given by Eq. (5) for any nonlinear function $b(x_1)$ such that there are as many scrolls as equilibrium points, regardless of whether the parameters of the system are the same ($\alpha_1 = \alpha_2 = \alpha_3$) or different ($\alpha_1 \neq \alpha_2 \neq \alpha_3$), as long as the system satisfies the conditions to be classified as UDS I.

Future work must be able to apply the obtained results to other systems to confirm the generality of the developed technique, or

otherwise implement new tools for predicting tipping points in dynamical systems without having to solve the systems of equations. Overall, this study advances our understanding of inflection points in dynamical systems and provides a solid foundation for future research in this field since the prediction of tipping points is critical in numerous contexts, from ecology to economics.

APPENDIX: ANGULAR EQUIVALENCE

Next we will develop an equivalent form to Eq. (11) to determine the angle between the manifolds.

Let $\vartheta_1 \in \mathbb{R}$ and $\vartheta_2 = \overline{\vartheta_3} \in \mathbb{C}$ are the eigenvectors of the matrix $\boldsymbol{M}$ given in (6). We define the vectors $\boldsymbol{v}_i = \mathrm{Re}\{\vartheta_i\}$ for $i = 1,2$ and form the set $V = \{\boldsymbol{v}_1, \boldsymbol{v}_2\}$. Let $\boldsymbol{\chi} = (\chi_1, \chi_2, \chi_3) \in \mathbb{R}^3$ be the equilibrium point of the system described by Eq. (1) for the region $\Omega_2 \subset \mathbb{R}^3$, and the parameter $\gamma_d^i \in \mathbb{R}$ defined as:

$$\gamma_d^i = \{\gamma \in \mathbb{R} : \chi_1 + \gamma v_{i1} = d\},$$

where $\boldsymbol{v}_i = (v_{i1}, v_{i2}, v_{i3}) \in V$. Then, the points A, B, C, and D illustrated in Figure 3 can be described as follows:

$$\begin{aligned} A &= \boldsymbol{\chi} + \gamma_{-1}^2 \boldsymbol{v}_2, \quad B = \boldsymbol{\chi} + \gamma_{+1}^1 \boldsymbol{v}_1, \\ C &= \boldsymbol{\chi} + \gamma_{+1}^2 \boldsymbol{v}_2, \quad D = \boldsymbol{\chi} + \gamma_{-1}^1 \boldsymbol{v}_1. \end{aligned} \tag{12}$$

Explicitly, the parameter can be obtained as follows:

$$\gamma_d^i = \frac{d - \chi_1}{v_{i1}},$$

and since the equilibrium point for the region Ω_2 is the origin, we have $\boldsymbol{\chi} = \mathbf{0} \in \mathbb{R}^3$. Thus, the parameters are:

$$\gamma_{-1}^i = \frac{-1}{v_{i1}}, \quad \gamma_{+1}^i = \frac{+1}{v_{i1}}, \tag{13}$$

where it can be observed that $\gamma_{+1}^i = -\gamma_{-1}^i, i = 1,2$.

If we use the same construction as in Eq. (9), but substitute the points from (12), we get the following:

$$\begin{aligned} &\boldsymbol{M}_s = \vec{DB} = D - B = (\boldsymbol{\chi} + \gamma_{-1}^1 \boldsymbol{v}_1) - (\boldsymbol{\chi} + \gamma_{+1}^1 \boldsymbol{v}_1) = \dots \\ &\gamma_{-1}^1 \boldsymbol{v}_1 - \gamma_{+1}^1 \boldsymbol{v}_1 = (\gamma_{-1}^1 - \gamma_{+1}^1)\boldsymbol{v}_1, \\ &\boldsymbol{M}_u = \vec{AC} = A - C = (\boldsymbol{\chi} + \gamma_{-1}^2 \boldsymbol{v}_2) - (\boldsymbol{\chi} + \gamma_{+1}^2 \boldsymbol{v}_2) = \dots \\ &\gamma_{-1}^2 \boldsymbol{v}_2 - \gamma_{+1}^2 \boldsymbol{v}_2 = (\gamma_{-1}^2 - \gamma_{+1}^2)\boldsymbol{v}_2. \end{aligned} \tag{14}$$

Substituting (13) into Eq. (14), we have that

$$\boldsymbol{M}_s = 2\gamma_{-1}^1 \boldsymbol{v}_1, \quad \boldsymbol{M}_u = 2\gamma_{-1}^2 \boldsymbol{v}_2. \tag{15}$$

Without loss of generality, let's assume that $\gamma_{-1}^1, \gamma_{-1}^2 > 0$, and therefore

$$\|\boldsymbol{M}_s\| = 2\gamma_{-1}^1 \|\boldsymbol{v}_1\|, \quad \|\boldsymbol{M}_u\| = 2\gamma_{-1}^2 \|\boldsymbol{v}_2\|. \tag{16}$$

To calculate the angle between the vectors $\boldsymbol{M}_s$ and $\boldsymbol{M}_u$, the dot product (denoted by $\cdot$) can be implemented as follows:

$$\boldsymbol{M}_s \cdot \boldsymbol{M}_u = \|\boldsymbol{M}_s\| \|\boldsymbol{M}_u\| \cos(\theta).$$

When substituting (15) and (16) into the above equation, you get:

$$(2\gamma_{-1}^1)(2\gamma_{-1}^2)(\boldsymbol{v}_1 \cdot \boldsymbol{v}_2) = (2\gamma_{-1}^1)(2\gamma_{-1}^2)\|\boldsymbol{v}_1\| \|\boldsymbol{v}_2\| \cos(\theta),$$

and therefore:

$$\cos(\theta) = \frac{1}{\langle \boldsymbol{v}_1 \rangle \langle \boldsymbol{v}_2 \rangle} \sum_{i \in \mathbb{I}} v_{1i} v_{2i},$$

where

$$\langle \boldsymbol{v}_j \rangle = \left(\sum_{i \in \mathbb{I}} v_{ji}^2 \right)^{1/2},$$

for $j = 1,2$ and with $\mathbb{I} \subseteq \{1,2,3\}$ a collection of indices. Note that $\langle \boldsymbol{v}_j \rangle \equiv \|\boldsymbol{v}_j\|$ when $\mathbb{I} = \{1,2,3\}$. Then the angle between vectors is defined by:

$$\cos(\theta_{\mathbb{I}}) = \frac{1}{\langle \boldsymbol{v}_1 \rangle \langle \boldsymbol{v}_2 \rangle} \left| \sum_{i \in \mathbb{I}} v_{1i} v_{2i} \right|.$$

Explicity, we will have:

$$\begin{aligned} \cos(\theta_{1,2}) &= \frac{|v_{11}v_{21} + v_{12}v_{22}|}{\sqrt{v_{11}^2 + v_{12}^2}\sqrt{v_{21}^2 + v_{22}^2}}, \\ \cos(\theta_{1,3}) &= \frac{|v_{11}v_{21} + v_{13}v_{23}|}{\sqrt{v_{11}^2 + v_{13}^2}\sqrt{v_{21}^2 + v_{23}^2}}, \\ \cos(\theta_{2,3}) &= \frac{|v_{12}v_{22} + v_{13}v_{23}|}{\sqrt{v_{12}^2 + v_{13}^2}\sqrt{v_{22}^2 + v_{23}^2}}, \\ \cos(\theta_{1,2,3}) &= \frac{|v_{11}v_{21} + v_{12}v_{22} + v_{13}v_{23}|}{\sqrt{v_{11}^2 + v_{12}^2 + v_{13}^2}\sqrt{v_{21}^2 + v_{22}^2 + v_{23}^2}}. \end{aligned} \tag{17}$$

Now suppose that the matrix M given in (6) has the eigenvalues $\lambda_1 = p \in \mathbb{R}$, and $\lambda_{2,3} = a \pm ib$ with $a, b \in \mathbb{R}$. Then the eigenvectors of the matrix M can be written as:

$$\begin{pmatrix} \vartheta_1, \vartheta_2, \vartheta_3 \end{pmatrix} = \begin{pmatrix} 1 & 1 & 1 \\ p & a - \mathrm{i}b & a + \mathrm{i}b \\ p^2 & -b^2 - 2\mathrm{i}ab + a^2 & -b^2 + 2\mathrm{i}ab + a^2 \end{pmatrix},$$

while their real part is as follows:

$$\begin{pmatrix} \boldsymbol{v}_1 & \boldsymbol{v}_2 \end{pmatrix} = \begin{pmatrix} 1 & 1 \\ p & a \\ p^2 & a^2 - b^2 \end{pmatrix}.$$

Substituting the aboved described into Eq. (17), we get:

$$\begin{aligned} \cos(\theta_{1,2}) &= \frac{|1+pa|}{\sqrt{1+p^2}\sqrt{1+a^2}}, \\ \cos(\theta_{1,3}) &= \frac{|1+p^2(a^2-b^2)|}{\sqrt{1+p^4}\sqrt{1+(a^2-b^2)^2}}, \\ \cos(\theta_{2,3}) &= \frac{|pa+p^2(a^2-b^2)|}{\sqrt{p^2+p^4}\sqrt{a^2+(a^2-b^2)^2}}, \\ \cos(\theta_{1,2,3}) &= \frac{|1+pa+p^2(a^2-b^2)|}{\sqrt{1+p^2+p^4}\sqrt{1+a^2+(a^2-b^2)^2}}. \end{aligned} \tag{18}$$

Regardless of which way is chosen, via eigenvectors as described in Eqs. (17) or using the eigenvalues as in Eqs. (18), analysis of these expressions when the parameter μ is varied yields the same plot as in Figure 6.

Acknowledgments

J.L.E.M. thanks CONAHCYT for financial support (CVU-706850), and to J.A.G. for the opportunity to do a postdoctoral fellowship at CICESE.

Availability of data and material

The data used to support the findings of the study are included within the article.

Conflicts of interest

The authors declare that there is no conflict of interest regarding the publication of this paper.

Ethical standard

The authors have no relevant financial or non-financial interests to disclose.

LITERATURE CITED

Anzo-Hernández, A., H. Gilardi-Velázquez, and E. Campos-Cantón, 2018 On multistability behavior of unstable dissipative systems. Chaos: An Interdisciplinary Journal of Nonlinear Science **28**: 033613.

Awal, N. M. and I. R. Epstein, 2021 Period-doubling route to mixed-mode chaos. Physical Review E **104**: 024211.

Biggs, R., S. R. Carpenter, and W. A. Brock, 2009 Turning back from the brink: detecting an impending regime shift in time to avert it. Proceedings of the National academy of Sciences **106**: 826–831.

Campos-Cantón, E., 2015 Switched systems based on unstable dissipative systems. IFAC-PapersOnLine **48**: 116–121.

Campos-Cantón, E., J. G. Barajas-Ramirez, G. Solis-Perales, and R. Femat, 2010 Multiscroll attractors by switching systems. Chaos: An Interdisciplinary Journal of Nonlinear Science **20**.

Chen, L., F. Nazarimehr, S. Jafari, E. Tlelo-Cuautle, and I. Hussain, 2020 Investigation of early warning indexes in a three-dimensional chaotic system with zero eigenvalues. Entropy **22**: 341.

Echenausía-Monroy, J., J. Cuesta-García, and J. Ramirez-Pena, 2022 The wonder world of complex systems. Chaos Theory and Applications **4**: 267–273.

Echenausía-Monroy, J., H. Gilardi-Velázquez, N. Wang, R. Jaimes-Reátegui, J. García-López, *et al.*, 2022a Multistability route in a pwl multi-scroll system through fractional-order derivatives. Chaos, Solitons & Fractals **161**: 112355.

Echenausía-Monroy, J., S. Jafari, G. Huerta-Cuellar, and H. Gilardi-Velázquez, 2022b Predicting the emergence of multistability in a monoparametric pwl system. International Journal of Bifurcation and Chaos **32**: 2250206.

Echenausía-Monroy, J. L., J. García-López, R. Jaimes-Reátegui, D. López-Mancilla, and G. Huerta-Cuellar, 2018 Family of bistable attractors contained in an unstable dissipative switching system associated to a snlf. Complexity **2018**.

Echenausía-Monroy, J. L., G. Huerta-Cuellar, R. Jaimes-Reátegui, J. H. García-López, V. Aboites, *et al.*, 2020 Multistability emergence through fractional-order-derivatives in a pwl multi-scroll system. Electronics **9**: 880.

Fang, S., S. Zhou, D. Yurchenko, T. Yang, and W.-H. Liao, 2022 Multistability phenomenon in signal processing, energy harvesting, composite structures, and metamaterials: A review. Mechanical Systems and Signal Processing **166**: 108419.

Gilardi-Velázquez, H. E., R. d. J. Escalante-González, and E. Campos-Cantón, 2018 Bistable behavior via switching dissipative systems with unstable dynamics and its electronic design. IFAC-PapersOnLine **51**: 502–507.

Gilardi-Velázquez, H. E., L. Ontañón-García, D. G. Hurtado-Rodriguez, and E. Campos-Cantón, 2017 Multistability in piecewise linear systems versus eigenspectra variation and round function. International Journal of Bifurcation and Chaos **27**: 1730031.

Guan, S., C.-H. Lai, and G. Wei, 2005 Bistable chaos without symmetry in generalized synchronization. Physical Review E **71**: 036209.

Jiang, J., A. Hastings, and Y.-C. Lai, 2019 Harnessing tipping points in complex ecological networks. Journal of the Royal Society Interface **16**: 20190345.

Jiang, J., Z.-G. Huang, T. P. Seager, W. Lin, C. Grebogi, *et al.*, 2018 Predicting tipping points in mutualistic networks through dimension reduction. Proceedings of the National Academy of Sciences **115**: E639–E647.

Jung, H. and J. W. Ager, 2023 A tipping point for solar production of hydrogen? Joule **7**: 459–461.

Keleş, Z., G. Sonugür, and M. Alçin, 2023 The modeling of the rucklidge chaotic system with artificial neural networks. Chaos Theory and Applications **5**: 59–64.

Kleiner, I., 2007 *A history of abstract algebra*. Springer Science & Business Media.

Lane, S. N., 2011 The tipping point: How little things can make a big difference. Geography **96**: 34–38.

Lenton, T. M., H. Held, E. Kriegler, J. W. Hall, W. Lucht, *et al.*, 2008 Tipping elements in the earth's climate system. Proceedings of the national Academy of Sciences **105**: 1786–1793.

Lohmann, J., D. Castellana, P. D. Ditlevsen, and H. A. Dijkstra, 2021 Abrupt climate change as a rate-dependent cascading tipping point. Earth System Dynamics **12**: 819–835.

Lorenz, E. N., 1963 Deterministic nonperiodic flow. Journal of atmospheric sciences **20**: 130–141.

Moghadam, N. N., R. Ramamoorthy, F. Nazarimehr, K. Rajagopal, and S. Jafari, 2022 Tipping points of a complex network biomass model: Local and global parameter variations. Physica A: Statistical Mechanics and its Applications **592**: 126845.

Moore, J. C., 2018 Predicting tipping points in complex environmental systems. Proceedings of the National Academy of Sciences **115**: 635–636.

Nazarimehr, F., S. Jafari, S. M. R. Hashemi Golpayegani, M. Perc, and J. C. Sprott, 2018 Predicting tipping points of dynamical systems during a period-doubling route to chaos. Chaos: An Interdisciplinary Journal of Nonlinear Science **28**.

Ott, E., 2002 *Chaos in dynamical systems*. Cambridge university press.

O'Regan, S. M., E. B. O'Dea, P. Rohani, and J. M. Drake, 2020 Transient indicators of tipping points in infectious diseases. Journal of the Royal Society Interface **17**: 20200094.

Peng, X., M. Small, Y. Zhao, and J. M. Moore, 2019 Detecting and predicting tipping points. International Journal of Bifurcation and Chaos **29**: 1930022.

Rial, J. A., R. A. Pielke, M. Beniston, M. Claussen, J. Canadell, *et al.*, 2004 Nonlinearities, feedbacks and critical thresholds within the earth's climate system. Climatic change **65**: 11–38.

Safavi, S. and P. Dayan, 2022 Multistability, perceptual value, and internal foraging. Neuron .

Scheffer, M., S. Carpenter, J. A. Foley, C. Folke, and B. Walker, 2001 Catastrophic shifts in ecosystems. Nature **413**: 591–596.

Tsakonas, S., M. Hanias, and L. Magafas, 2022 Application of the moving lyapunov exponent to the s&p 500 index to predict major

declines. Journal of Risk .
Wunderling, N., A. von der Heydt, Y. Aksenov, S. Barker, R. Bastiaansen, *et al.*, 2023 Climate tipping point interactions and cascades: A review. EGUsphere **2023**: 1–45.

How to cite this article: Echenausía-Monroy, J. L., Cuesta-García, J.R., Gilardi-Velázquez, H.E., Muni, S.S., and Alvarez-Gallegos, J. Predicting Tipping Points in a Family of PWL Systems: Detecting Multistability via Linear Operators Properties *Chaos Theory and Applications*, 6(2), 73-82, 2024.